Effects Of Magnetic Interaction Of Acoustic Waves In A Combustion MHD Generator

Author(s): T. D. Simons, R. H. Eustis, and M. Mitchner

Session Name: Open Cycle II

SEAM: 19 (1981)

SEAM EDX URL: https://edx.netl.doe.gov/dataset/seam-19

EDX Paper ID: 850

EFFECTS OF MAGNETIC INTERACTION ON ACOUSTIC WAVES IN A COMBUSTION MHD GENERATOR*

T. D. Simons, R. H. Eustis, and M. Mitchner
High Temperature Gasdynamics Laboratory
Stanford University
Stanford, California

Abstract

A one-dimensional linearized theory using integral transforms has been used to predict the growth and attenuation of waves. The theory is applicable for weak magnetic interaction and is useful for initial conditions in large generators or to characterize the phenomena in laboratory scale facilities. The wave growth predictions are obtained by perturbing the normal acoustic wave solutions with the effect of magnetic interaction. In order to make the predictions, one-dimensional models of the generalized electrical configuration for an MHD channel were developed, and include implicitly some two-and three-dimensional effects such as boundary layer and electrode phenomena. The theory predicts that non-ideal boundary layer effects may significantly reduce the growth rates. For the Stanford M-2 facility, the theory predicts that waves should experience small, but not insignificant, amounts of attenuation.

I. Introduction

In practice there are many sources of inherent unsteadiness in an MHD generator, including poor mixing and incomplete combustion of the reactants, turbulence, variation of the flow conditions, and possible changes in the load circuit. These non-uniformities and fluctuation in the plasma may themselves cause a degradation of the steady-state performance of the MHD generator [1], [2]. In an ordinary fluid without magnetic interaction, small variations in fluid properties can propagate as ordinary acoustic and entropy waves. Magnetic interaction modifies the propagation of the waves. Variations in the pressure and temperature, such as might be associated with the propagating waves, cause a variation in the plasma properties, such as the electrical conductivity and the Hall parameter. For a combustion-driven MHD facility, the electrical conductivity is a strong function of temperature ($d \log\sigma / d \log T \approx 13$), and the Hall parameter is a moderate function of the fluid density. The changes in these properties then affect the electric fields and currents. These fluctuations affect the fluid properties by changing the body force on the gas ($\vec{J} \times \vec{B}$) and by Joule heating ($\vec{J} \cdot \vec{E}'$). Thus fluctuations in the fluid properties, propagating as waves, interacting with the electric and magnetic fields, can under certain circumstances either add or dissipate energy in the flowing plasma. Adding energy to the propagating waves can produce an instability, increasing the amplitude of the travelling waves. These increased disturbances can exacerbate the problems due to non-uniformities previously mentioned, and cause additional problems. Because large current and electric field fluctuations are associated with the property fluctuations, the load circuit, particularly the inverters, may experience high level transients, which could result in damage. In addition high temperatures can affect the heat transfer rates, and high pressures can threaten the structural integrity of the MHD channel itself. It is important therefore, to understand the effects and behavior of these waves.

In combustion MHD generators the plasma can be characterized as an equilibrium, partially-ionized, electrically neutral, low magnetic Reynolds number plasma. Several investigators have considered the possibility of instabilities with can propagate under such conditions [3]-[9].

Most recently, Barton (1979) [10] has conducted a thorough investigation of magneto-acoustic and magneto-entropic waves in combustion MHD facilities. Barton used the linearized MHD equations to examine the propagation of waves in an MHD generator with arbitrary axial and transverse load circuits, and included, in an approximate fashion, the variation of steady-state property gradients, in addition to the dependence of the plasma properties on the thermodynamic state. The results of his calculations indicate that in facilities with large interaction significant amplification of travelling waves could occur in ideal Faraday, Hall, and diagonal wall generators over a wide range of load factors.

Experimental investigation of the behavior of magneto-acoustic waves has been quite limited. A lengthy study of fluctuations in MHD generators was performed by Dicks, Scott, and colleagues [11]-[13]. They measured fluctuations in electrode current, axial-electrode voltage, and plasma luminosity in a combustion-driven, supersonic diagonal conducting-wall facility. These measurements were analysed statistically and showed no evidence of magneto-acoustic wave growth. Most recently Barton, [14]-[15] has performed a broad study of fluctuations in a subsonic, combustion driven MHD generator. Barton measured the inherent fluctuations in channel pressure, voltages from internal voltage pins, and current in the load circuit, as a function of DC current, with and without a B-field. In both studies however, the size of the facilities and the magnitude of magnetic interaction were small in comparison to proposed base-load facilities.

The applicability of the previous theories to operating MHD generators is limited by the assumption, in each case, of ideal electrical performance, where boundary layer and near electrode phenomena are neglected. These non-ideal phenomena are especially important in smaller facilities, such as those previously used to examine magneto-acoustic phenomena. This paper describes an analytical model of

*Supported by U.S. Department of Energy under Contract DE-AC01-80ET15611.

magneto-acoustic phenomena which identifies the dependence of wave growth and dispersion of single disturbances with the plasma properties and load conditions of non-ideal MHD generators, utilizing a quasi-one-dimensional model of the generalized electrical configuration, which incorporates some two-and three-dimensional phenomena, including a model of voltage drop as a function of current density. In particular it is observed that wave growth rates can be strongly influenced by the resistance associated with boundary layer voltage drops.

The paper first describes a new model for obtaining closed-form solutions for wave growth rates of an arbitrary property disturbance in a generator of weak interaction. Then the quasi-one-dimensional model is described briefly, and applied to predict growth rates in the Stanford facility, with the aim to investigate the existence of the mechanisms which can cause magneto-acoustic instabilities. Finally, the results and features of these predictions are discussed.

II. Magneto-Acoustic Theory

Consider an ideal MHD generator with arbitrary axial and transverse load circuits, with external batteries permitted in the load circuits as shown in Fig. 1. Following Barton [10], the one-dimensional, time-dependent, constant area MHD equations can be written as:

$$\frac{(1+M_P)}{P}\frac{DP}{Dt} - \frac{(1-M_T)}{T}\frac{DT}{Dt} + \frac{\partial u}{\partial x} = 0 \qquad (1)$$

$$\rho\frac{Du}{Dt} + \frac{\partial P}{\partial x} = (\vec{J} \times \vec{B})_x \qquad (2)$$

$$\rho c_v \frac{DT}{Dt} + P\frac{\partial u}{\partial x} = \frac{\vec{J}\cdot\vec{J}}{\sigma} \qquad (3)$$

where

$$\frac{D}{Dt} = \frac{\partial}{\partial t} + u\frac{\partial}{\partial x} . \qquad (4)$$

Here P, T, and u have been chosen as the dependent variables. The density is eliminated in the usual continuity equation by assuming a perfect gas, $P = \rho RT/\hat{M}$, and permitting a variable molecular weight $\hat{M}$ so that

$$M_T = \frac{T_o}{\hat{M}_o}\left(\frac{\partial \hat{M}}{\partial T}\right)_P \quad \text{and} \quad M_p = \frac{P_o}{\hat{M}_o}\left(\frac{\partial \hat{M}}{\partial P}\right)_T .$$

This variation is included because the chemical composition of a combustion MHD plasma is a moderate function of temperature and pressure. A low magnetic Reynolds number and a single temperature plasma are assumed, and heat transfer and viscosity are neglected in the core.

The method of solution to the system of Eqs. (1 - 3) is outlined as follows:

1. The MHD equations are linearized by assuming small disturbances to the steady state property values of the form

$$\xi(x,t) = \xi_o + \xi'(x,t) .$$

2. The linearized equations for ξ' are Fourier transformed in space, then Laplace transformed in time to yield an algebraic system of equations for the transformed variables.

3. The system is solved and the transforms are inverted for the case of no magnetic interaction and no current, yielding the normal acoustic solution.

4. The perturbation to the normal acoustic solution is calculated to show the effect of magnetic interaction on the waves.

The MHD Eqs. (1-3) are linearized and normalized, yielding

$$P'_t + M_o P'_x - \frac{(1-M_T)}{(1+M_p)}[T'_t + M_o T'_x] + \frac{1}{(1+M_p)} u'_x = 0 \qquad (5)$$

$$\frac{1}{\gamma_o} P'_x + u'_t + M_o u'_x = \left(\frac{L}{\rho_o a_o^2}\right)(\vec{J} \times \vec{B})'_x \qquad (6)$$

$$(\gamma_o - 1) u'_x + T'_t + M_o T'_x = \left(\frac{L}{\rho_o c_{vo} T_o a_o}\right)\frac{\vec{J}\cdot\vec{J}}{\sigma} \qquad (7)$$

A list of normalized variables is given in Table 1. The characteristic length scale L can be associated with the channel length. The "source" terms in (6) and (7) are evaluated from the electrical equations that relate $(\vec{E}, \vec{J})$ to the plasma properties and the fluid variables (P, T, u) [see next section]. Included in the source terms are the dependence of electrical conductivity and Hall parameter in a linear fashion on pressure and temperature. It is these dependencies which can lead to instabilities. The source terms also include terms in the dependent variables P', T' and u'.

The fluid fluctuations are assumed to be zero at distances far away from the part of the MHD channel under consideration, and to have an arbitrary initial value inside the channel. The boundary and initial conditions may therefore be written as follows:

$$\text{B.C.} \quad P'(\pm\infty,t) = T'(\pm\infty,t) = u'(\pm\infty,t) = 0 \qquad (8)$$

$$\text{I.C.} \quad P'(x,0) = P_I(x),\ T'(x,0) = T_I(x),\ u'(x,0) = u_I(x) \qquad (9)$$

The initial conditions are restricted to functions which vanish at the boundaries, $\pm\infty$, and are absolutely integrable. The effect of solving the problem on an infinite domain is to restrict the solution to only one pass of the wave through the generator. Because of the wave nature of the solutions, the solutions to the infinite domain problem and finite domain problem are identical until such time as a wave reaches a boundary. The solution on the infinite domain does not account for reflection at the boundaries that would result in an actual facility.

Utilizing Eqs. (8 & 9), the Eqs. (1-3) are first Fourier transformed, then Laplace transformed to yield the linear algebraic system,

$$(a_{ij} - S_o c_{ij})\,\hat{\tilde{\xi}}'_j = b_i \,, \tag{10}$$

where

$$\hat{\tilde{\xi}}'_j = \begin{bmatrix} \hat{\tilde{P}}' \\ \hat{\tilde{T}}' \\ \hat{\tilde{u}}' \end{bmatrix} \tag{11}$$

denotes the doubly-transformed perturbation quantities.

The coefficients a_{ij} and b_i are not dependent on the electrical configuration of the generator. The c_{ij} include the effects of magnetic interaction, and are found by perturbing the steady-state MHD terms in Eqs. 1-3. A general method for determining these coefficients and the steady-state generator performance is developed in [16].

The linear system, Eq. (10) can be easily solved for $\hat{\tilde{P}}'$, $\hat{\tilde{T}}'$, and $\hat{\tilde{u}}'$. In principle, these expressions can be inverted by contour integration in the s- and τ- complex planes, but an informative and useful solution can be obtained when the interaction parameter, S_o, is small. In general the double transforms can be inverted to yield

$$\xi'_j(\bar{x},\bar{t}) = \sum_{k=1}^{3} \int_{-\infty}^{\infty} f_k(A_k,s)\, \exp[2\pi i s\bar{x} + A_k\bar{t}]\; ds \,. \tag{12}$$

The $f_k(A_k)$ are functions of the poles of the determinant of Eq. [10], A_k, and the integration represents the inversion of the Fourier Transform.

When $S_o = 0$, the A_k are given by

$$A_{k0} = -2\pi i s C_k \tag{13}$$

where the C_k are the normalized wave speeds,

$$C_{1,2} = M_o \pm \mu_o,\quad C_3 = M_o \tag{14}$$

where

$$\mu_o^2 = \frac{1 + (\gamma_o - 1)\,(1-M_T)}{\gamma_o(1+M_p)} \tag{15}$$

The result of the inversion when $S_o = 0$ thus gives undamped traveling waves with the velocities given by the C_k. This is the normal acoustic result. (For operating MHD facilities, $\mu_o \approx 1.02$. Thus the effect of permitting variable molecular weight is to slightly alter the wave speeds of the upstream and downstream moving acoustic waves.) Recalling that the speeds are normalized on the sonic velocity, a_o, one sees that $C_{1,2}$ correspond to waves with velocities $u_o \pm a_o$, and that C_3 is a convective wave with a real velocity u_o.

Now, a perturbation due to magnetic interaction is allowed in the A_k of the form

$$A_k = A_{k0} + S_o(-2\pi i s \varepsilon_k + \delta_k) + 0(S_o^2) \tag{16}$$

It is seen that the ε_k represent perturbations in the wave speeds, and the δ_k represent exponential growth factors [$\exp(S_o \delta k t)$], if they are purely real. Making this substitution for the A_k in Eq. (12) and comparing terms of similar order gives the results:

1. $\varepsilon_1 = \varepsilon_2 = \varepsilon_3 = 0$ (17)

   There is no first order perturbation to the wave speeds.

2. For the growth factors, the δ_k are all purely real functions of the coefficients in Eq. [10]. Hence, a positive value for the δ_k indicates wave growth, a negative value indicates attenuation. Using these values for the ε_k and δ_k, Eq. (12) can be evaluated to give the solutions to lowest order in S_o,

$$\xi'_j(\bar{x},\bar{t}) = \sum_{k=1}^{3} [\alpha^P_{0jk} P_I(\bar{x}-C_k\bar{t}) + \alpha^T_{0jk} T_I(\bar{x}-C_k\bar{t}) + \alpha^u_{0jk}\, u_I(\bar{x}-C_k\bar{t}) + 0(S_o)]\, \exp(S_o\delta_k\bar{t}) \tag{18}$$

   where the α^f_{0jk} are given in Table 2. Each of the three ξ'_j consists of three independent traveling waves, traveling with the velocities given by the C_k, with the indicated exponential growth factor. The initial amplitudes are a linear combination of the initial conditions. For simplicity, the first order effects in the initial amplitudes have been neglected as higher order with respect to the α^f_{0jk} terms, consistent with the approximation. Details of these first order terms have been calculated separately [16].

As S_o goes to zero, the normal acoustic solutions are recovered from Eq. (10). The principal effect of the magnetic interaction is to add an exponential growth term to the solution. Observe that the growth factor is the same for all waves which move at the same wave speed. Figure 2 shows schematically the propagation of the pressure, temperature, and velocity waves resulting from a disturbance in the dependent variables at one common location. It is observed from the α^f_{0jk} that the initial temperature disturbance does not contribute to the pressure and velocity waves. The temperature waves which travel with the P' and u' waves are isentropic in normal acoustics. Only the temperature wave moves with the fluid velocity. This wave is often called the entropy wave in normal acoustics because entropy is convected with this wave.

III. Quasi-One-Dimensional Electrical Model

The perturbation analysis is especially suited to facilities of weak interaction, including laboratory scale generators or larger generators operating at low current densities. In order to characterize the electrical performance of such facilities a quasi-one-dimensional model of the general electrical configuration of an MHD gnerator has been developed, [16] which includes arbitrary axial and transverse load circuits with possible current augmentation and the effects of boundary layers and near electrode voltage drops, as shown in Fig. 1. The models' predictions of steady-state performance are perturbed for small property disturbances, in order to determine the coefficients c_{ij} in Eq. (10).

Important assumptions of the model include infinitely-fine segmentation, slow variation in the axial properties, and that the direction of the current is constant in the core region of the channel. The latter assumption evidences itself in 2D calculations, even with finite segmentation [8]. The analysis shows that the boundary layer voltage drops can be regarded as effective resistances in the load circuits, which can be calculated from a model of electrical model of electrical conductivity in the boundary layer or deduced from voltage drop data. The suitability of the electrical model to the Stanford M2 facility was assessed by comparing predictions of Faraday current with the measurements of Barton [10]. Voltage drop data simultaneously recorded on internal voltage pins allow calculation of the boundary layer resistance. Predicted and experimental current densities for representative M2 operating conditions agree well, as shown in Figures 3a and 3b. To some extent the agreement is expected because of the use of experimental data for the boundary layer voltage drops, but these voltage drops can represent only a small fraction of the total transverse load resistance, which controls the current level. At low external load factors the boundary layer resistances are 20-50% of the total, depending on Mach number , and at higher load factors they are much lower.

IV. Wave Growth Rates

The good agreement between theory and experiment for the current densities provides a basis for using the non-ideal theory to also predict wave growth rates in the M-2 facility. For conditions typical of the M-2 channel, the perturbation analysis is well suited for determining wave growth rates in the M-2 facility. Experimental observations of waves in the M-2 channel support the conjecture that the waves are only weakly disturbed. Growth rate predictions were made for each of the three wave types for the Faraday configuration with voltage augmentation in the transverse load circuit of 120v and 240v, and for a range of Mach numbers.

Wave growth rates for one pass through the Stanford M-2 channel are predicted as a function of external load factor with Mach number as a parameter. The external load factor is the load factor that would exist in an idealized facility (i.e. without boundary layer voltage drops), as determined by the external load resistors. The ideal load factor is zero with short circuit across the electrodes and unity at open circuit. Here

$$K_{\text{external, Faraday}} = \frac{\bar{R}_s}{1+\bar{R}_s} \qquad (19)$$

1. Downstream moving waves (Speed $M_o + \mu_o$), Figs. 4a and 4b.

   For both values of voltage augmentation, little change would be observed in the downstream waves. At highest augmentation, a maximum 1% growth is observed at higher load factors, and a maximum 5% attenuation at achievable current levels at lower load factors. (The maximum current density is about 1.5 Amps/cm^2. Above this level, significant erosion of the electrodes occurs). These small growth rates are believed too small to measure in the M-2 facility.

2. Upstream moving waves (Speed $M_o + \mu_o$), Figs. 5a and 5b.

   At both levels of augmentation, the upstream moving waves attenuate more than the downstream moving waves because of longer residence time in the channel. Over the range of achievable current density levels, 5 - 15% attenuation is predicted, with the larger values corresponding to the higher Mach numbers.

3. Convective (entropy waves) (Speed M_o), Figs. 6a and 6b.

   With 120v augmentation, as much as 20% attenuation is observed in the entropy waves. With 240v augmentation, 30-80% attenuation is predicted at achievable current levels, with the higher value corresponding to lower Mach numbers where the wave residence time is longer. These levels of attenuation should be observable in the M-2 Facility.

The values of the wave growth rates calculated as described above, differ considerably from idealized values obtained by neglecting the boundary layer drops. Figure 7 shows growth rates for the convected wave with 240v augmentation without accounting for boundary layer losses. In this case the theory predicts that the convected waves in a segmented Faraday generator are always amplified when the plasma resistance is less than the load resistance (load factor of 0.5).

Because of the limitations of the perturbation analysis, which considers the effects of weak magnetic interaction, the proposed theory has only a limited application to large facilities [18]. However, if waves in a large facility increase at the initial rates predicted by the present theory, they would experience significant growth, as also predicted by of Barton. In proposed MHD facilities, the resistive voltage drops may be small compared to the plasma core resistance, because of hot slag layers and Joule heating, and these generators may therefore be more susceptible to magneto-acoustic interaction and wave growth.

V. Conclusions

Predictions of magneto-acoustic instabilities are strongly affected by the electrical resistance in electrode boundary layers. The application of a new magneto-acoustic model, which incorporates these effects suggests that wave growth rates are greatly reduced when the boundary layer resistances are comparable in magnitude to the resistance of the plasma core, which is typically only a few ohms. In small facilities, the model predicts that waves might experience small but not insignificant amounts of attenuation, where ideal theories have predicted some amplification.

An experimental program is continuing to study these effects by temporally resolved measurements of voltage, current, pressure, and luminosity disturbances associated with single wave pulses.

An efficient method of creating distinct single wave pulses within a MHD generator by discharging a charged capacitor through existing electrodes has been modelled and also confirmed experimentally.

References

1. Rosa, R. J., "The Hall and Ion Slip Effects in a Nonuniform Gas", Phys. Fluids 5, 1080, (Sept. 1962).

2. McCune, J. E., "Non-linear Effects of Fluctuations on MHD Performance", AVCO-Everett Research Lab Research Report 205, (January 1965).

3. Velikov, E. P., "Hall Instability of Current Carrying Slightly-Ionized Plasmas", Symp. MPD Electrical Power Generation, Newcastle-upon-Tyne, G. B., 135, (1962).

4. Wright, J. K., "A Temperature Instability in MHD Flow", Proc. Phys. Soc. 81, 498, (1963).

5. McCune, J. E. "Wave Growth and Instability in Partially-Ionized Gases", Intl. Symp. on MHD Electrical Power Generation, Paris, Paper 33, (1964).

6. Sutton, G. W. and Witalis, E. A., "Linearized Analysis of MHD Generator Flow Stability", Intl. Symp. on MHD Electrical Power Generation, Paris, (1964).

7. Locke, E. V. and McCune, J. E., "Growth Rates for Axial Magneto-Acoustic Waves in a Hall Generator", AIAA Journal 4, 1748, (Oct. 1966).

8. Oliver, D. A., "The Time Dependent MHD Generator", MIT Gas Turbine Lab Report No. 115, (March 1974).

9. Powers, W. L. and Dicks, J. B., "Transient Wave Growth in MGD Generators", AIAA Journal 6, 1007, (June 1968).

10. Barton, J. B., "Fluctuations in Combustion-Driven MHD Generators", Ph. D. Thesis, Stanford University (1980).

11. Dicks, J. B., Wu, Y.C.L, Scott, M. H., and Murray, E. M. "Fluctuations in Series Connected Open Cycle MHD Generators", Proc. of the Fifth Intl. Conference on MHD Electrical Power Generation, Munich, (1971).

12. Scott, M. A., Kornstett, K., and Dicks, J. B., "Evidence of Fluctuation and Absence of Instabilities in Open Cycle MHD Generators", Thirteenth Symposium on Engineering Aspects of MHD, Stanford, (1973).

13. Scott, M. A., "An Experimental Investigation of Fluctuations in a Direct Coal-Fired Open Cycle MHD Generator and a Method for Modelling these Fluctuations", AIAA Paper No. 76-313, (1976).

14. Barton, J. P., Koester, J. K., and Mitchner, M., "An Experimental Investigation of Fluctuating Properties Within a Combustion MHD Generator", Sixteenth Symposium on Engineering Aspects of MHD, Pittsburg, (1977).

15. Barton, J. P., Koester, J. K., and Mitchner, M., "Fluctuations in Combustion-Driven MHD Generator Systems", Eighteenth Symposium on Engineering Aspects of MHD, Butte, (1979).

16. T. D. Simons, "Effects of Magnetic Interaction on Acoustic Waves in a Combustion MHD Generator", thesis proposal, High Temperature Gasdynamics Laboratory, Stanford University, October 1980.

17. Oliver, D. A. "Nonuniform Electrical Conduction in Magneto-hydrodynamic Channels", SU-IPR Report No. 163, Stanford University (May 1967).

18. "A High Magnetic Field MHD Generator Program," Quarterly Report on Contract No. DE-AC01-80ET15611, FE-15611-4, Stanford University, January 1981.

Table 1. Normalized Variables Introduced in the Magneto-Acoustic Analysis

$\bar{x} = x/L$ $u' = u_1/a_o$

$\bar{t} = ta_o/L$

$P' = P_1/P_o$

$T' = T_1/T_o$

$S_o = \frac{\sigma_o B_o^2 L}{\rho_o a_o}$, interaction parameter (perturbation variable)

M_o = Mach number

L = Generator axial length

$\bar{J}_y = J_y/\sigma_o a_o B_o$

Table 2. Coefficients for Eq. 18, the α^f_{0jk}

j	k \ f	P	T	u
1	1	$\frac{1}{2}$	0	$\frac{\mu_o \gamma_o}{2}$
	2	$\frac{1}{2}$	0	$-\frac{\mu_o \gamma_o}{2}$
	3	0	0	0
2	1	$-\frac{(\gamma_o-1)}{2\gamma_o \mu_o^2}$	0	$\frac{(\gamma_o-1)}{2\mu_o}$
	2	$-\frac{(\gamma_o-1)}{2\gamma_o \mu_o^2}$	0	$-\frac{(\gamma_o-1)}{2\mu_o}$
	3	$\frac{(\gamma_o-1)}{\gamma_o \mu_o^2}$	1	0
3	1	$\frac{1}{2\gamma_o \mu_o}$	0	$\frac{1}{2}$
	2	$\frac{-1}{2\gamma_o \mu_o}$	0	$\frac{1}{2}$
	3	0	0	0

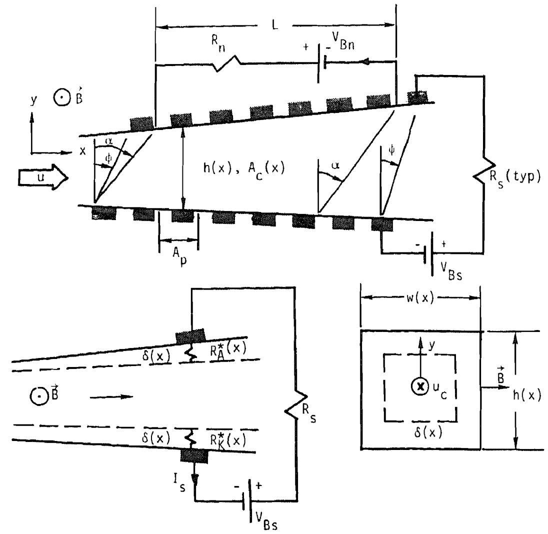

Fig. 1 A representation of the MHD generator used in the non-ideal quasi-one-dimensional model with generalized electrical connections and boundary layers.

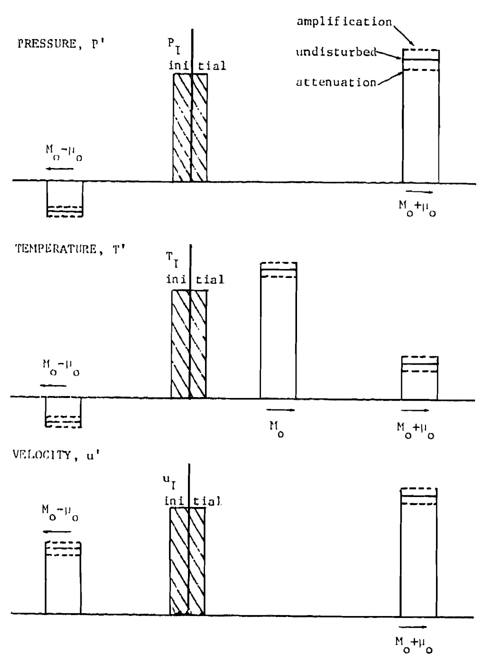

Fig. 2 A schematic representation of propagation of the three waves ($M_o \pm \mu_o, M_o$) for each of the dependent variables P', T', and U' at some time $t > 0$. Shaded pulses represent initial conditions of each wave at the same location.

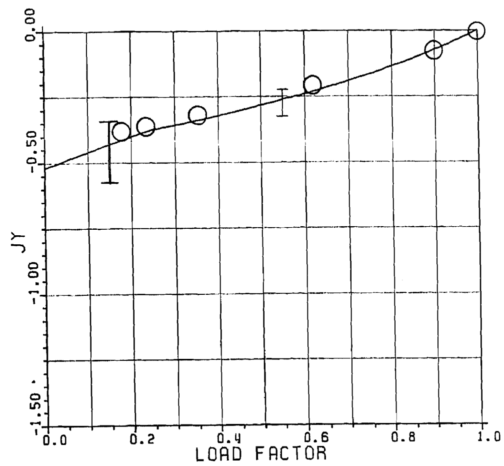

(a) V_{Bs} = 120 V

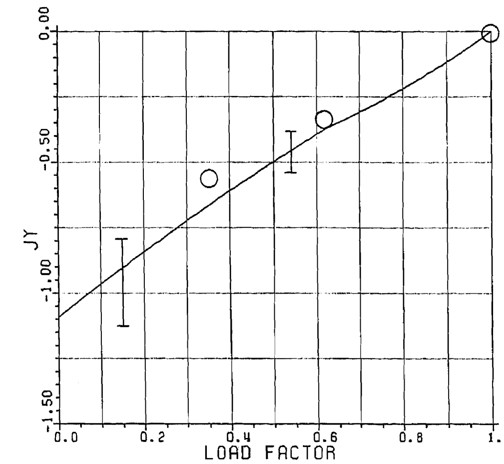

(b) V_{Bs} = 240 V

Fig. 3 Comparison of the data of Barton (circles) and predictions of the quasi-one-dimensional model for the transverse current density in a Faraday generator M_o = 0.3. Error bars reflect the uncertainty in voltage drop measurements and boundary layer thickness.

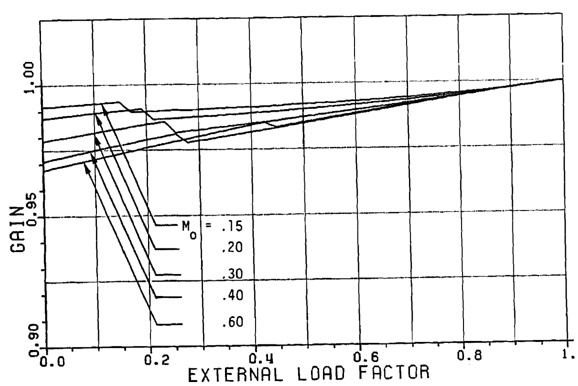

(a) V_{Bs} = 120 V

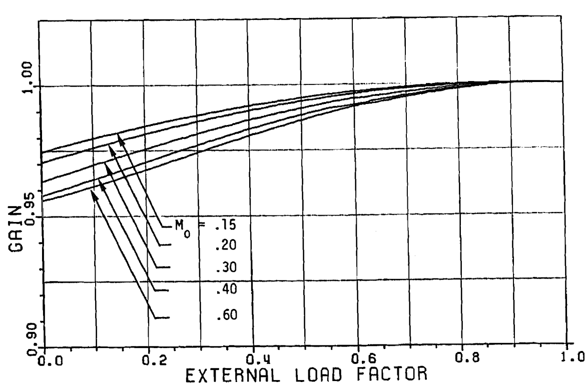

(b) V_{Bs} = 240 V

Fig. 4 Predicted wave growth for a downstream moving acoustic wave traveling the length of the Stanford M2 facility, Faraday configuration.

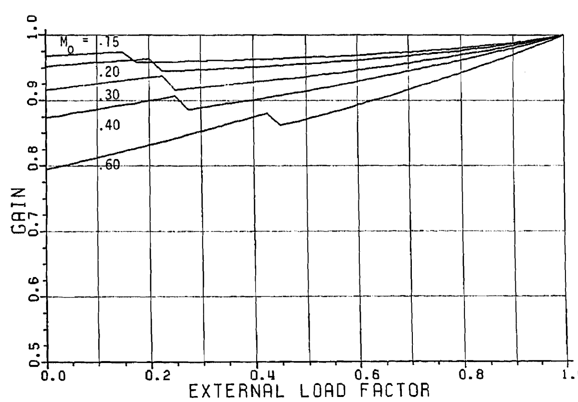

(a) V_{Bs} = 120 V

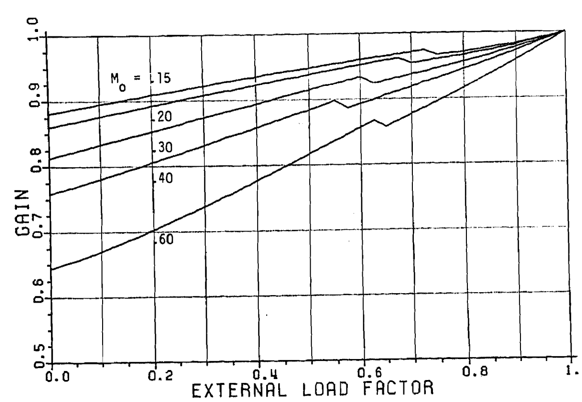

(b) V_{Bs} = 240 V

Fig. 5 Predicted wave growth for an upstream moving acoustic wave traveling the length of the Stanford M2 facility, Faraday configuration.

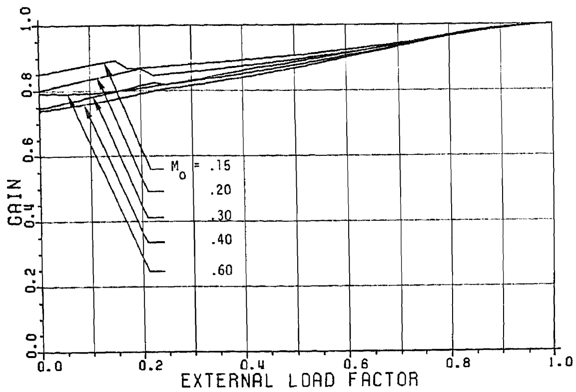

(a) V_{Bs} = 120 V

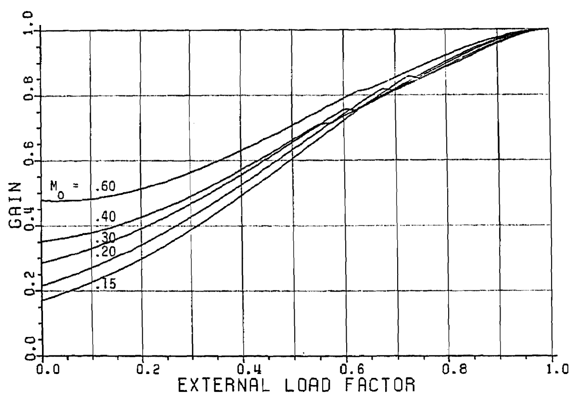

(b) V_{Bs} = 240 V

Fig. 6 Predicted wave growth for a convected (entropy) wave traveling the length of the Stanford M2 facility, Faraday configuration.

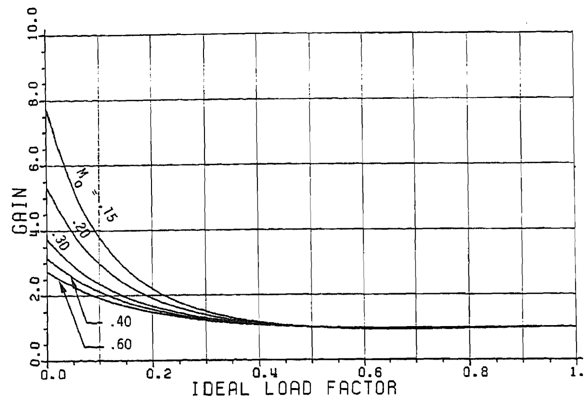

Fig. 7 Predicted wave growth for a convected (entropy) wave traveling the length of the Stanford M2 facility using an idealized electrical model with 240 V augmentation in the Faraday configuration. (cf. Figure 6b).